Effect of guide field on three dimensional electron shear flow instabilities in collisionless magnetic reconnection

Neeraj Jain[1, 2] and Jörg Büchner[1, 2]

[1)] *Max Planck/Princeton Center for Plasma Physics, Göttingen, Germany*

[2)] *Max Planck Institute for Solar System Research, Justus-Von-Liebig-Weg-3, Göttingen, Germany*

arXiv:1411.3213v2 [physics.plasm-ph] 6 Apr 2015

We examine the effect of an external guide field and current sheet thickness on the growth rates and nature of three dimensional unstable modes of an electron current sheet driven by electron shear flow. The growth rate of the fastest growing mode drops rapidly with current sheet thickness but increases slowly with the strength of the guide field. The fastest growing mode is tearing type only for thin current sheets (half thickness $\approx d_e$, where $d_e = c/\omega_{pe}$ is electron inertial length) and zero guide field. For finite guide field or thicker current sheets, fastest growing mode is non-tearing type. However growth rates of the fastest 2-D tearing mode and 3-D non-tearing mode are comparable for thin current sheets ($d_e <$half thickness $< 2\,d_e$) and small guide field (of the order of the asymptotic value of the component of magnetic field supporting electron current sheet). It is shown that the general mode resonance conditions for electron-magnetohydrodynamic (EMHD) and magnetohydrodynamic (MHD) tearing modes depend on the effective dissipation mechanism (electron inertia and resistivity in cases of EMHD and MHD, respectively). The usual tearing mode resonance condition ($\mathbf{k}.\mathbf{B}_0 = 0$, $\mathbf{k}$ is the wave vector and $\mathbf{B}_0$ is equilibrium magnetic field) can be recovered from the general resonance conditions in the limit of weak dissipation. Necessary conditions (relating current sheet thickness, strength of the guide field and wave numbers) for the existence of tearing mode are obtained from the general mode resonance conditions.

I. INTRODUCTION

Magnetic reconnection is a plasma process in which topological changes of magnetic field lines release the energy stored in magnetic field in the form of kinetic energy and heat. It is considered to be the cause of the release of magnetic energy in solar flares, sub-storms in Earth's magnetosphere, sawtooth crashes in tokamaks and many astrophysical systems, e.g., accretion disk. The topological changes of magnetic field lines take place in a current sheet and require dissipation in the current sheet. In the absence of collisions, lack of dissipation allows the current sheet to thin down to microscopic scales, such as, electron and ion inertial lengths, and an effective dissipation is provided by micro-physical plasma processes. As a result, the reconnecting current sheet develops a two scale structure (along its thickness), viz., an electron current sheet with thickness of the order of an electron inertial length, $d_e = c/\omega_{pe}$ embedded inside an ion current sheet with thickness of the order of an ion inertial length, $d_i = c/\omega_{pi}$. Reconnection of field lines takes place in electron current sheets and couples to ion and then further to very large MHD scales.

The electron and ion current sheets are susceptible to a variety of instabilities. These instabilities have potential to affect the rate and structure of reconnection. The role of ion scale instabilities in reconnection has been discussed in a review by Büchner and Daughton (2006)[1]. On electron scales, the electron current sheet (ECS) can be unstable to electro-magnetic instabilities driven by the gradients in the ECS or to electrostatic Buneman[2] instability driven by relative drift of electrons and ions. The electrostatic Buneman instability grows (typical growth rates $\sim$ fraction of ω_{pe}) much faster than the electro-magnetic instabilities without affecting magnetic fields. Growth of the electro-magnetic tearing and non-tearing instabilities leads to the generation of flux ropes/plasmoids[3,4] and filamentation of the ECS[5], respectively. The conditions under which an ECS filaments or generates flux ropes/plasmoids depend on the presence of an external guide field and thickness of the current sheet. Recently it was shown that, depending upon thickness of the ECS, Electron Shear Flow Instabilities (ESFI) can grow both as 3-D oblique tearing modes which generate flux ropes/plasmoids and/or non-tearing modes which filament the ECS[6,7]. Without an external guide field, the tearing mode instability dominates over non-tearing modes only if the sheet is thin, with half thickness close to an electron inertial length[6,7]. Otherwise non-tearing mode instabilities dominate.

In this paper, we perform linear stability analysis for ESFI of an ECS in the presence of an external guide field. We employ an electron-magnetohydrodynamic (EMHD)[8] model. Studies of electron shear flow instabilities in EMHD approximation have earlier been reported but without guide field[9–15]. These instabilities have also been referred as current driven sausage and kink instabilities, because, in EMHD electron flow is equivalent to current[10,12,13].

In the next section we briefly describe electron-magnetohydrodynamic model and obtain the linearized EMHD equations for ESFI. Section III discuss effects of guide field on ESFI. Necessary conditions for the existence of EMHD tearing mode are obtained in Section IV. We conclude this paper in section V.

II. ELECTRON-MHD MODEL

Electron-magnetohydrodynamic (EMHD) model is a fluid model for electron dynamics in a stationary background of ions. It is valid for spatial scales smaller than d_i and time scales smaller than ω_{ci}^{-1}. In EMHD, electron dynamics is described by electron momentum equation coupled with Maxwell's equations. An evolution equation for magnetic field $\mathbf{B}$ can be obtained by eliminating electric field from the electron momentum equation using Faraday's law[8].

$$\frac{\partial}{\partial t}(\mathbf{B} - d_e^2\nabla^2\mathbf{B}) = \nabla \times [\mathbf{v}_e \times (\mathbf{B} - d_e^2\nabla^2\mathbf{B})], \tag{1}$$

where, $\mathbf{v}_e = -(\nabla \times \mathbf{B})/\mu_0 n_0 e$ is electron fluid velocity. In addition to ignoring the ion dynamics, Eq. (1) assumes uniform electron number density n_0 and incompressibility of the electron fluid. The displacement current is ignored under the assumption $\omega << \omega_{pe}^2/\omega_{ce}$. In EMHD, the frozen-in condition of magnetic field breaks down due to the electron inertia (which is contained in the definition of $d_e \propto \sqrt{m_e}$). In the absence of electron inertia ($d_e \to 0$), Eq. (1) represents the condition that magnetic field is frozen in the electron fluid.

The equilibrium magnetic field is taken to be $\mathbf{B}_0 = B_{y0}\tanh(x/L)\hat{y} + B_{z0}\hat{z}$ corresponding to a current density $\mathbf{J}_0 = (B_{y0}/\mu_0 L)\mathrm{sech}^2(x/L)\hat{z}$, where L is the half thickness of the electron current sheet. For stationary ions, electron fluid velocity is related to current density by the relation $\mathbf{J} = -n_0 e\mathbf{v}_e$. In the limit of cold electrons, bipolar electrostatic electric field co-located with the electron current sheet balances the Lorentz force in the current sheet. Small deviations from charge neutrality in the electron current sheet can support the bipolar

electric field[16]. This force balance is different from the force balance between pressure gradient and Lorentz force as in the case of a Harris current sheet. The bipolar electrostatic electric field and the new force balance in electron current sheet have been observed in particle-in-cell simulations[16,17], laboratory experiments[18], and space observations[19]. EMHD equations linearized about this equilibrium can be written as,

$$d_e^2\frac{d^2v_x}{dx^2}-(1+k^2d_e^2)v_x=-\frac{d_e^2\omega_{ce}^2}{B_{y0}^2}\frac{F-d_e^2F''}{\bar{\omega}}b_x-\frac{d_e^2\omega_{ce}^2}{B_{y0}^2}\frac{F(F-d_e^2F'')}{\bar{\omega}^2}v_x + \frac{k_z(v_0-d_e^2v_0'')}{\bar{\omega}}v_x \quad (2)$$

$$d_e^2\frac{d^2b_x}{dx^2}-(1+k^2d_e^2)b_x=\frac{F-d_e^2F''}{\bar{\omega}}v_x \quad (3)$$

where $\bar{\omega}=\omega-k_zv_0$, $k^2=k_y^2+k_z^2$, $\omega_{ce}=eB_{y0}/m_e$ and $F=\mathbf{k}.\mathbf{B}_0$. The perturbed x-components of electron flow velocity (v_x) and magnetic field (b_x) are Fourier transformed in y, z, and t. The sub-script 'e' is dropped from electron flow velocity and a prime ($'$) over an equilibrium variable denotes derivative with respect to x. Equations (2) and (3) are solved for confined eigen functions v_x and b_x corresponding to eigen frequency ω which is related to k_y , k_z , L and B_{z0} by a dispersion relation. Results are presented in normalized variables. The magnetic field is normalized by B_{y0} , length by the electron inertial length d_e , time by the inverse electron cyclotron frequency $\omega_{ce}^{-1}=(eB_{y0}/m_e)^{-1}$, and velocity by the electron Alfven velocity $v_{Ae}=d_e\omega_{ce}$. Under this normalization, $\mathbf{J}=-\mathbf{v}_e$ holds.

III. TEARING AND NON-TEARING ELECTRON SHEAR FLOW INSTABILITIES

We define an unstable mode to be tearing mode if (1) v_x is an odd function of x at some position $x=x_0$ (inside the ECS) so that $v_x(x_0)=0$ and (2) $b_x(x_0)\neq 0$. All other modes are considered non-tearing type. Note that the free energy source for all the unstable modes (both tearing and non-tearing) is electron shear flow which is equivalent to electric current for stationary ions.

Growth rates in k_y-k_z space for various values of L and B_{z0} are shown in Fig. 1. For a fixed value of current sheet thickness, the domain of unstable modes shift to smaller values of k_z. The growth rates $L>d_e$ are significantly affected even for small guide field. On the

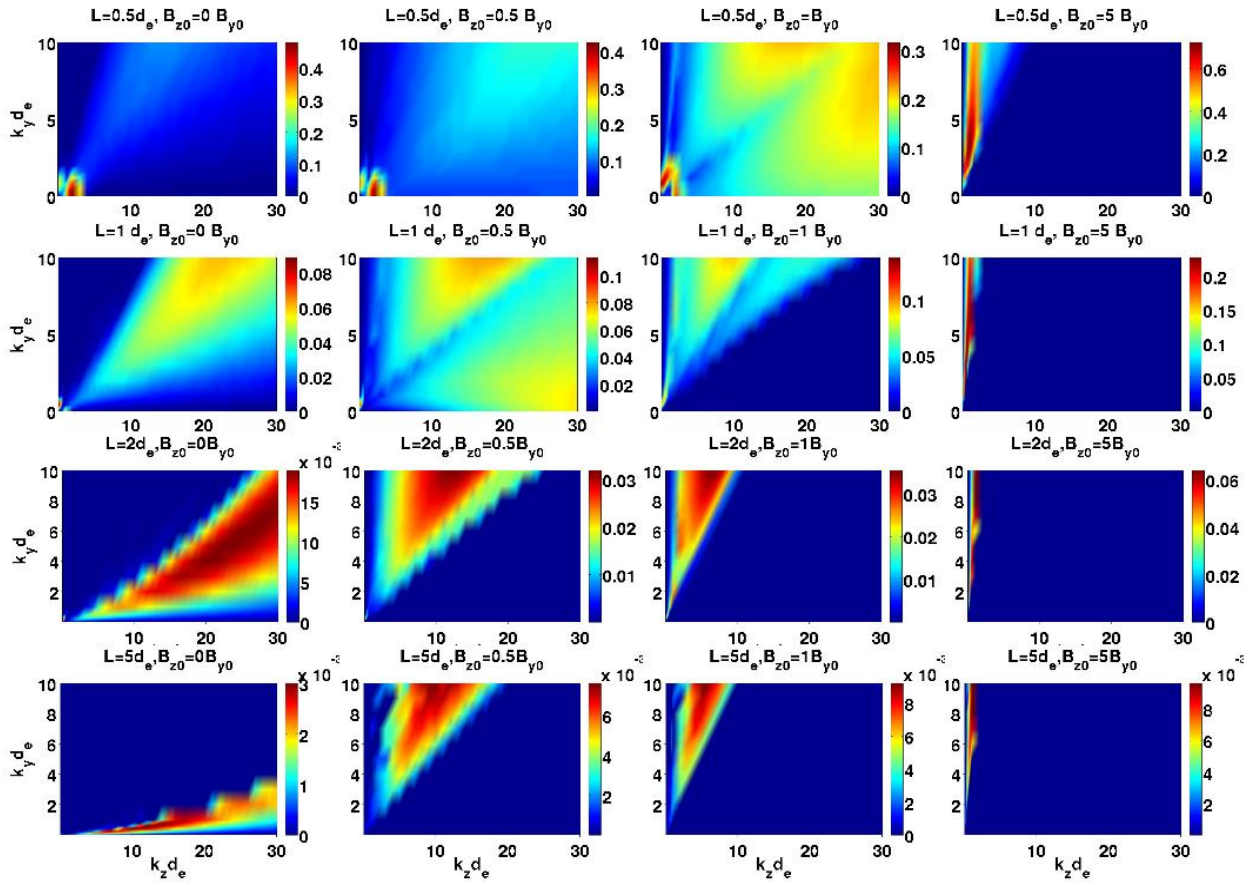

FIG. 1. Growth rates γ/ω_{ce} (color) of ESFI in k_y-k_z space for $L/d_e = 0.5$, 1.0, 2.0 and 5.0 (along column). For each value of L, $B_{z0}/B_{y0} = 0$, 0.5, 1.0 and 5.0. (along row).

other hand growth rates for $L < d_e$ are not affected much when strength of the guide field is small. This behavior is expected as Lorentz force terms in electron momentum equation are negligible in the limit $L << d_e$. It can also be shown that Eqs. (2) and (3) becomes independent of guide field in this limit. In the limit of $L << d_e$, $F - d_e^2 F'' \approx -d_e^2 k_y B_{y0}/L^2$is independent of guide field. Therefore guide field appears only in the expression for $F = k_y B_{y0} + k_z B_{z0}$ in the second last term on the RHS of Eq. (2). In the limit $L << d_e$, this term can be neglected in comparison to the last term on RHS of Eq. 2, thus making Eqs. (2) and (3) independent of the guide field.

The maximum growth rate drops rapidly with L for a given value of the guide field. The maximum growth rate increases slowly as the guide field is increased for fixed current sheet thickness except for $L = 0.5\, d_e$ (in Fig. 1) for which maximum growth rate first drops and then increases. An electron shear flow instability whose growth rate increases with the

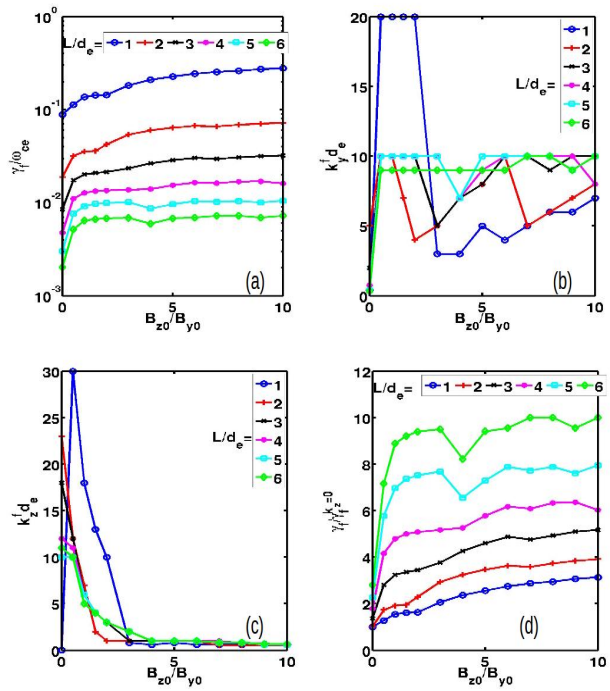

FIG. 2. Growth rates γ_f (a), wave numbers k_y^f (b) and k_z^f (c) of the fastest growing mode as functions of guide field B_{z0} for various current sheet thicknesses. In (d), ratio $\gamma_f/\gamma_f^{k_z=0}$, where $\gamma_f^{k_z=0}$ is the growth rate of the fastest 2-D ($k_z = 0$) tearing mode, as a function of the guide field.

strength of the guide field was also reported in 3-D particle-in-cell simulations of electron current sheet[5]. The variation of the growth rate (γ_f) of the fastest growing mode (maximum growth rate in k_y-k_z space) with the strength of the guide field for various values of L is shown in Fig. 2a. The rate of increase of the growth rate is faster for weak strength of the guide field ($B_{z0}/B_{y0} < 1$) as compared to the rate for large guide field ($B_{z0}/B_{y0} > 5$). In between the fast and slow rise of the growth rate with guide field, a plateau forms. The rate of the fast rise of γ_f for weak guide field is higher for large values of L while opposite is true for the slow increase for strong guide field. The range of the guide field values for the plateau depends on L.

The wave numbers, k_y^f and k_z^f, of the fastest growing mode are shown in Figs. 2b and 2c. The wavenumber k_y^f takes a jump to large values as soon as the guide field becomes finite and remains at this value for a range of the values of guide field. On further increasing the guide field, k_y^f drops to rise again. This trend of variation of k_y^f with the guide field can be seen for all values of L. The jump in the value of k_y^f is the largest for $L = d_e$. The wave

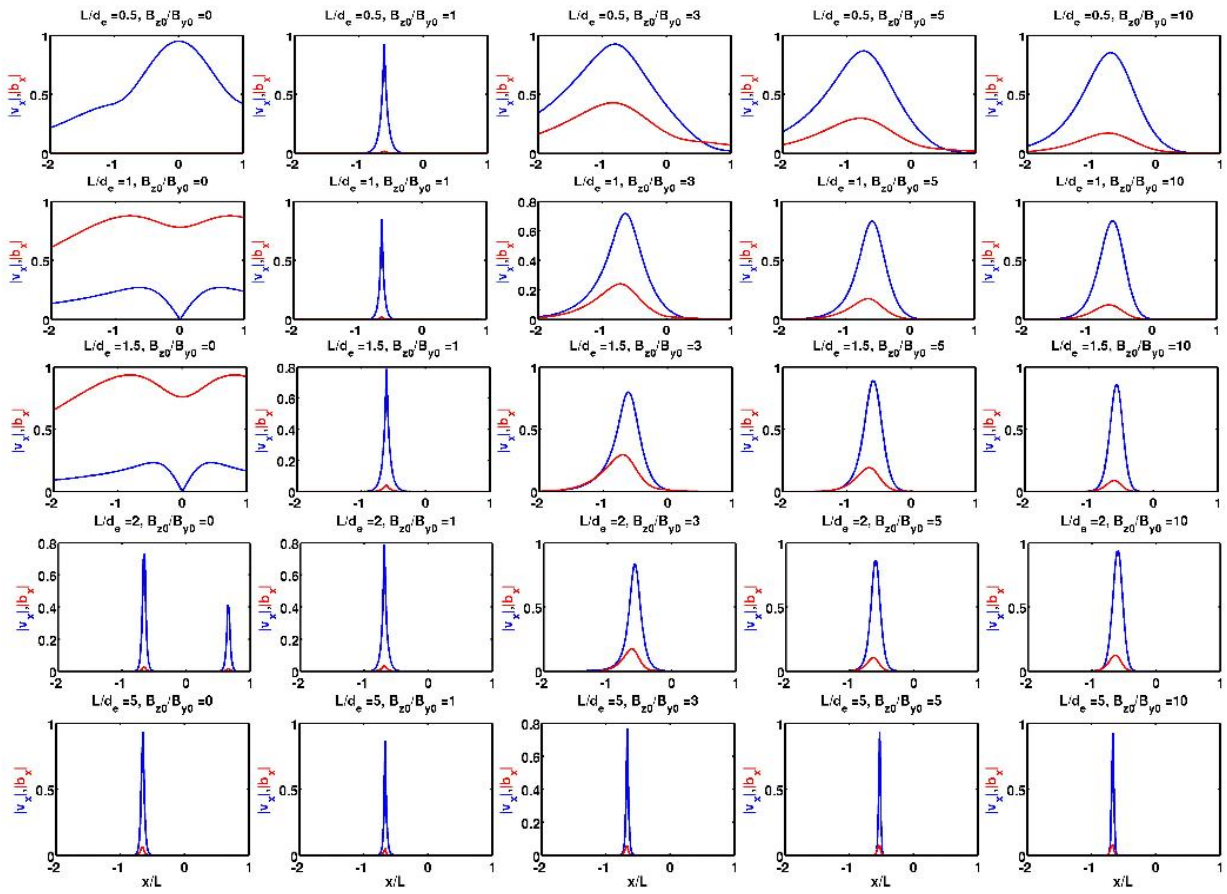

FIG. 3. Absolute values of complex eigen functions v_x (blue) and b_x (red) corresponding to the fastest growing mode for $L/d_e = 0.5, 1, 1.5, 2$ and 5 (varying along a column), and $B_{z0}/B_{y0} = 0, 1, 3, 5$ and 10 (varying along a row). Horizontal axis is in units of L and shows only a small region in x.

number k_z^f has large jump as soon as guide field becomes finite only for $L = d_e$. After the initial jump k_z^f drops. For $L > d_e$, k_z^f drops with increasing guide field. For all values of L, k_z^f saturates at $k_z^f d_e \approx 1$ for large values of guide field. The sudden changes in γ_f, k_y^f and k_z^f as soon as guide field becomes finite indicate that the inclusion of guide field triggers a new kind of unstable mode different from tearing mode.

In order to distinguish between tearing and non-tearing modes, we plot absolute values of complex eigen functions v_x and b_x of the fastest growing mode in Fig. 3. For tearing mode, x-component of magnetic field (B_x) and velocity (V_x) in real space should be finite and zero, respectively, at the mode rational surface. These components can be expressed as $B_x = \mathrm{Re}[|b_x| \exp(i\theta_b + ik_y y + ik_z z - i\omega t)]$ and $V_x = \mathrm{Re}[|v_x| \exp(i\theta_v + ik_y y + ik_z z - i\omega t)]$, where

$\tan(\theta_v) = \mathrm{Im}(v_x)/\mathrm{Re}(v_x)$ and $\tan(\theta_b) = \mathrm{Im}(b_x)/\mathrm{Re}(b_x)$. In Fig. 3, $|v_x| = 0$ and $|b_x| \neq 0$ (and therefore so for V_x and B_x) only for $L/d_e = 1$ and 1.5 and $B_{z0} = 0$. Therefore tearing mode is the fastest growing mode in a very small range of $L - B_{z0}$ parameter space.

Although the fastest growing mode is non-tearing in the presence of finite guide field, 2-D tearing mode ($k_z = 0$) is not affected by the guide field because guide field disappears from eigen value Eqs. (2) and (3) for $k_z = 0$. For $L = d_e$ and $B_{z0} = B_{y0}$, growth rate of the fastest 2-D tearing mode ($k_y d_e = 0.4$) is comparable to that of the fastest growing 3-D non-tearing mode (Fig. 1). In order to determine the relative importance of the tearing and non-tearing modes as a function of L and B_{z0}, we compare the growth rate of the fastest 3-D mode (γ_f) and that of the fastest 2-D ($k_z = 0$) tearing mode ($\gamma_f^{k_z=0}$) in Fig. 2d. The ratio $\gamma_f/\gamma_f^{k_z=0}$ increases with both the current sheet thickness and the strength of the guide field. For zero guide field, the ratio $\gamma_f/\gamma_f^{k_z=0}$ is of the order of unity (varies from 1-3 for L/d_e =1-6). The ratio increases with the strength of the guide field but remain order of unity for thinner current sheets ($L/d_e = 1$ and 2) for guide field as large as $B_{z0}/B_{y0} = 10$. The initial rate of increase of the ratio with guide field is larger for thicker current sheets. Therefore the ratio increases to much larger values even for $L > 2\,d_e$. It is expected that tearing mode can grow simultaneously with the non-tearing modes for thin current sheets and small value of guide field.

IV. NECESSARY CONDITIONS FOR EMHD TEARING MODE

Applying the tearing mode conditions, viz., $v_x(x_0) = 0$ and $b_x(x_0) \neq 0$, in Eqs. (2) and (3), we get necessary conditions for the existence of tearing eigen functions.

$$[\mathbf{k}.\mathbf{B}_0 - \mathbf{k}.\mathbf{B}_0'']_{x=x_0} = 0, \tag{4}$$

$$\left[\frac{1}{b_x}\frac{d^2 b_x}{dx^2}\right]_{x=x_0} = 1 + k^2, \tag{5}$$

where we have used $[d^2 v_x/dx^2]_{x=x_0} = 0$ as v_x is an odd function about $x = x_0$. Eqs. (4) and (5) are only necessary conditions for the existence of tearing type eigen functions which could either be stable or unstable. Since RHS of Eq. 5 is always finite, $b_x(x_0)$ and $[d^2 b_x/dx^2]_{x_0}$ can not be zero, except when both $b_x(x_0)$ and $[d^2 b_x/dx^2]_{x_0}$ approach zero simultaneously.

Eq. (4) is the mode resonance condition for EMHD tearing mode. Note that this condition is different from the usual resonance condition ($\mathbf{k}.\mathbf{B}_0 = 0$) for tearing mode. It reduces to

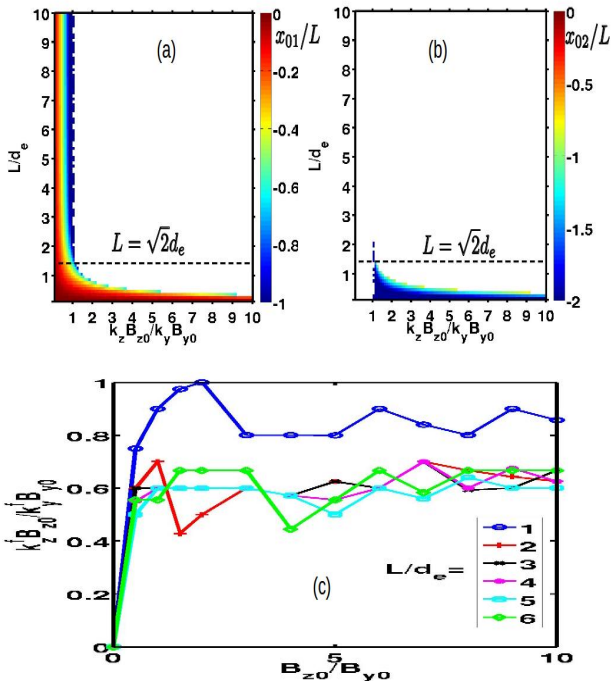

FIG. 4. Real roots x_{01}/L (a) and x_{02}/L (b) of Eq. (7). Color scales are saturated at $x_{01}/L = -1$ and $x_{02}/L = -2$. No real root exists in the white regions in L-$k_z B_{z0}/k_y$ space. In (c), quantity $k_z^f B_{z0}/k_y^f B_{y0}$ for the fastest growing modes obtained from the solutions of Eqs. (2) and (3) is plotted as a function of guide field for various values of current sheet thickness.

$\mathbf{k}.\mathbf{B}_0 = 0$ only for equilibrium scale length much larger than electron inertial length. In fact mode resonance condition for MHD tearing mode should also be different from $\mathbf{k}.\mathbf{B}_0 = 0$. This can be seen by applying conditions for tearing mode eigen functions in Eq. (14) of Furth et al.[20] Assuming uniform density, we get for MHD

$$\mathbf{k}.(\mathbf{B}_0 - L_\eta^2 \mathbf{B}_0'') = 0 \tag{6}$$

where $L_\eta = \eta/4\pi\omega$ is the resistive scale length and η is the resistivity. Eq. 6 reduces to $\mathbf{k}.\mathbf{B}_0 = 0$ only when equilibrium scale length is much larger than the resistive scale length.

Now we obtain some conditions on the existence of EMHD tearing mode from mode resonance condition Eq. (4). Substituting for the equilibrium magnetic field $\mathbf{B}_0$ in Eq. (4), the values of x_0 can be obtained from following equation.

$$\tanh^3\left(\frac{x_0}{L}\right) - \left(1 + \frac{L^2}{2}\right)\tanh\left(\frac{x_0}{L}\right) - \frac{k_z B_{z0} L^2}{2k_y} = 0 \tag{7}$$

For zero guide field, $B_{z0} = 0$, only real solution of Eq. (7) is $x_0 = 0$, as is expected. For finite guide field, x_0 can have non-zero values except for $k_z = 0$. One of the three roots of Eq. (7) is complex everywhere in the L-$k_z B_{z0}/k_y$ parameter space. The other two roots x_{01} and x_{02} have real values in regions of the L-$k_z B_{z0}/k_y$ parameter space and are plotted in Fig. 4. There exist no real solution in the parameter space $L > \sqrt{2}d_e$ and $k_z B_{z0}/k_y > 1$. In the limit $L >> \sqrt{2}d_e$ and $k_z B_{z0}/k_y >> 1$, Eq. (7) reduces to $\tanh^3(x_0/L) = k_z B_{z0} L^2/2k_y$ which has no real solution because $\tanh(x_0/L) \leq 1$. When $k_z B_{z0}/k_y < 1$, real solutions of x_0 exist for any value of L. In this limit, value of x_{01}/L does not depend on L for $L >> \sqrt{2}d_e$ but does depend on $k_z B_{z0}/k_y$. For $L >> \sqrt{2}d_e$ and $k_z B_{z0}/k_y < 1$, Eq. (7) can be simplified by neglecting the cubic term to give $x_0/L = -\tanh^{-1}(k_z B_{z0}/k_y)$ which is independent of L. This result can be derived from the condition $\mathbf{k}.\mathbf{B}_0 = 0$ which can be obtained from the resonance condition, Eq. (4), in the limit $L >> d_e$. In Fig. 4, $x_{01}/L < 0.6$ for $L < \sqrt{2}d_e$ and cubic term in Eq. 7 can be neglected giving,

$$\tanh\left(\frac{x_{01}}{L}\right) = -\frac{k_z B_{z0}}{k_y}\frac{L^2/2}{L^2/2+1}. \tag{8}$$

Eq. (8) can have real solutions for x_{01} as long as the RHS ≤ 1 which is satisfied for $k_z B_{z0}/k_y \leq 1$ for any $L < \sqrt{2}d_e$. For $k_z B_{z0}/k_y > 1$, real x_0 exists only if L is sufficiently small. For this reason, range of the values of L which allow real x_{01} shrinks with increasing $k_z B_{z0}/k_y > 1$. When $k_z B_{z0}/k_y \to 1$ and $L > \sqrt{2}d_e$, $|x_{01}|/L \gg 1$ pushing mode rational surface out of the electron current sheet.

The resonance condition, Eq. (4), is only a necessary condition for the existence of tearing eigen functions. Therefore it can not be used with certainty to predict the existence of tearing instability. However, its violation guarantees that tearing mode can not exist. The conditions for the non-existence of tearing mode can be stated as follows.

$$\frac{k_z B_{z0}}{k_y} > 1, \text{ if } L > \sqrt{2}d_e \tag{9}$$

$$> 1 + 2/L^2, \text{ if } L < \sqrt{2}d_e \tag{10}$$

Fig. 4c shows that value of the quantity $k_z B_{z0}/k_y B_{y0}$ calculated for the fastest growing remains smaller than unity even for those value of L and B_{z0} for which the fastest mode is non-tearing. This is not in contrast to the conditions stated above as $\mathbf{k}.(\mathbf{B}_0 - \mathbf{B}_0'') = 0$ is only a necessary condition for the existence of tearing mode.

V. CONCLUSION AND DISCUSSION

We have performed linear stability analysis of three dimensional electron shear flow instabilities of an ECS. The unstable domain of wave numbers shifts towards smaller values of k_z with the increasing strength of the guide field. The wave number k_z^f (along the direction of guide field) of the fastest growing mode drops with guide field and saturates at $k_z^f d_e \approx 1$ for large guide field. The growth rate of the fastest mode drops rapidly with current sheet thickness but increases slowly with the strength of the guide field. On examining the eigen functions of unstable modes we found that the fastest growing mode is no longer tearing mode for finite guide field even for thin current sheets ($L \approx d_e$). However growth rate of the fastest 2-D ($k_z = 0$) tearing mode is comparable to the growth rate of the fastest mode for thin current sheets ($1 < L/d_e < 2$) for small guide field. Therefore, in the nonlinear evolution of thin current sheets with a small guide field both tearing and non-tearing modes are expected to grow. For thicker current sheets the growth rate of the fastest 2-D tearing mode is much smaller than the fastest mode and thus the evolution is expected to be dominated by non-tearing mode. However, in cases where reconnection is driven from boundaries, the evolution may be dominated by tearing mode even for large guide field and thicker current sheets.

A general mode resonance condition, $\mathbf{k}.(\mathbf{B}_0 - \mathbf{B}_0'')$, for EMHD tearing mode was obtained. It was shown that the general resonance condition for MHD tearing mode, $\mathbf{k}.\mathbf{B}_0 - L_\eta^2 \mathbf{B}_0''$, is different from the usual resonance condition $\mathbf{k}.\mathbf{B}_0 = 0$. However the general resonance condition for EMHD (MHD) tearing mode reduces to $\mathbf{k}.\mathbf{B}_0 = 0$ if equilibrium scale length is much larger than the electron inertial length (resistive scale length). Necessary conditions for existence of tearing mode were obtained. These conditions relate wave numbers, current sheet thickness and strength of the guide field.

ACKNOWLEDGMENTS

This work was supported by Max-Planck/Princeton Center for Plasma Physics at the Max Planck Institute for Solar System Research, Justus-von-Liebig-Weg-3, Göttingen, Germany. We thank Dr. Bernhardt Bandow for his help to numerically optimize the EMHD code.

REFERENCES

[1]J. Büchner and W. S. Daughton, "Role of current aligned instabilities," In Reconnection of Magnetic Fields, 144(2006), j. Birn and E. R. Priest eds. Cambridge: Cambridge university press.

[2]O. Buneman, "Instability, turbulence and conductivity in current-carrying plasmas," Phys. Rev. Lett. **1**, 8 (1958).

[3]W. Daughton, V. Roytershteyn, H. Karimabadi, L. Yin, B. J. Albright, B. Bergen, and K. J. Bowers, "Role of electron physics in the development of turbulent magnetic reconnection in collisionless plasmas," Nature Physics **7**, 539 (2011).

[4]S. Markidis, P. Henri, G. Lapenta, A. Divin, M. Goldman, D. Newman, and E. Laure, "Kinetic simulations of plasmoid chain dynamics," Phys. Plasmas **20**, 082105 (2013).

[5]H. Che, J. F. Drake, and M. Swisdak, "A current filamentation mechanism for breaking magnetic field lines during reconnection," Nature **474**, 184 (2011).

[6]Neeraj Jain and J. Büchner, "Three dimensional instabilities of an electron scale current sheet in collisionless magnetic reconnection," Phys. Plasmas **21**, 062116 (2014).

[7]Neeraj Jain and J. Büchner, "Nonlinear evolution of three-dimensional instabilities of thin and thick electron scale current sheets: Plasmoid formation and current filamentation," Phys. Plasmas **21**, 072306 (2014).

[8]A. S. Kingsep, K. V. Chukbar, and V. V. Yan'kov, *Reviews of Plasma Physics*, Vol. 16 (Consultants Bureau, New York, 1990) p. 243.

[9]S. V. Basova, S. A. Varentsova, A. V. Gordeev, A. V. Gulin, and V. Yu. Shuvaev, "Inertial electron instability in low-density current-carrying plasmas," Fiz. Plazmy **17**, 615 (1991).

[10]A. Das and P. Kaw, "Nonlocal sausage-like instability of current channels in electron magnetohydrodynamics," Phys. Plasmas **8**, 4518 (2001).

[11]J. F. Drake, R. G. Kleva, and M. E. Mandt, Phys. Rev. Lett. **73**, 1251 (1994).

[12]N. Jain, A. Das, P. Kaw, and S. Sengupta, "Nonlinear electron magnetohydrodynamic simulations of sausage-like instability of current channels," Phys. Plasmas **10**, 29 (2003).

[13]Neeraj Jain, Amita Das, and Predhiman Kaw, "Kink instability in electron magnetohydrodynamics," Phys. Plasmas **11**, 4390 (2004).

[14]Neeraj Jain, Amita Das, Sudip Sengupta, and Predhiman Kaw, "Nonlinear electron-magnetohydrodynamic simulations of three dimensional current shear instability," Phys.

Plasmas **19**, 092305 (2012).

[15]Gurudatt Gaur and Amita Das, "Linear and nonlinear studies of velocity shear driven three dimensional electron-magnetohydrodynamics instability," Phys. Plasmas **19**, 072103 (2012).

[16]B. Li and R. Horiuchi, "Electron force balance in steady collision-less driven reconnection," Phys. Rev. Lett. **101**, 215001 (2008).

[17]L. J. Chen, William Daughton, B. Lefebvre, and Roy B. Torbert, "The inversion layer of electric fields and electron phase-space-hole structure during two-dimensional collisionless magnetic reconnection," Phys. Plasmas **18**, 012904 (2011).

[18]J. Yoo, M. Yamada, H. Ji, and C. E. Myres, "Observation of ion acceleration and ion heating during collisionless magnetic reconnection in a laboratory plasma," Phys. Rev. Lett. **110**, 215007 (2013).

[19]L. J. Chen, N. Bessho, B. Lefebvre, H. Vaith, A. Asnes, O. Santolik, A. Fazakerley, P. A. Puhl-Quinn, A. Bhattacharjee, Y. Khotyaintsev, P. Daly, and R. Torbert, "Multispacecraft observations of the electron current sheet, neighboring magnetic islands, and electron acceleration during magnetotail reconnection," Phys. Plasmas **16**, 056501 (2009).

[20]Harold P. Furth, John Killeen, and Marshal N. Rosenbluth, "Finite resistivity instabilities of a sheet pinch," Phys. Fluids **6**, 459 (1963).